A new strain-based method to determine GTN parameters for thin stainless steel foil

IOP Conf. Series: Journal of Physics: Conf. Series **1063** (2018) 012150 doi:10.1088/1742-6596/1063/1/012150

A new strain-based method to determine GTN parameters for thin stainless steel foil

P Zhang[1], M Pereira[2], B Rolfe[2], D Wilkosz[3], B Abeyrathna[1], M Weiss[1]

[1] Institute for Frontier Materials, Deakin University, Waurn Ponds, Pigdons Rd.,VIC 3216, Australia
[2] School of Engineering, Deakin University, Waurn Ponds, Pigdons Rd., VIC 3216, Australia
[3] Research and Innovation Center, Ford Motor Company, Dearborn, 2101 Village Rd., MI 48121, USA.

Email: pen@deakin.edu.au

Abstract. In this work, tensile tests were carried out on the 316L foil with a thickness of 0.1mm to calibrate the Gurson–Tvergaard–Needleman (GTN) model. Two calibration methods were compared for calibrating the same test data. The common approach is to use iterative finite element simulations to fit the experimental load-displacement curve. A new strain-based approach, which uses strain data obtained by a Digital Image Correlation (DIC) system, is presented here. It uses a stress-return-mapping algorithm to reconstruct the fracture related state variable, i.e., the accumulated void volume fraction. Fracture is predicted when the critical void fraction is reached at the measured fracture moment. The study shows that the new approach gives similar fracture model parameters compared to the common method, but with significantly higher computational efficiency.

1. Introduction

Stainless steel foil sheet is applied widely in manufacturing micro-forming products, such as bipolar plates in fuel-cells or micro-devices in the aerospace sector. Several studies used the finite element analysis (FEA) methods to predict the forming behaviour of copper foil [1] while only limited numerical investigations focused on stainless steel foil. To determine the ductile fracture of stainless steel foil, the Abaqus built-in Gurson–Tvergaard–Needleman (GTN) fracture model is used in this study. In general, the accuracy of a simulation model largely depends on the material model which is generally calibrated by experimental tests using inverse analysis [2]. Therefore the strategy is to minimize the difference between the experimental and the simulation results which can be in form of load-displacement or stress-strain relationships. The simulation is iteratively continued until the optimum is achieved. This approach is called FEA updating method. Several optimization algorithms [3] have been investigated in a large body of early works and some have been integrated in the commercial optimization packages such as LS-OPT, Isight and Hyperstudy. The parameter identification process for the updating method is time consuming [4]. One way to shorten the computational effort and time required is by using the Digital Image Correlation (DIC) technique to determine elasto-plastic parameters [5, 6]. In this semi-analytical method, the measured full-field strain field is input during the optimization, and herein massive cumbersome simulation can be avoided. Different from the full-field strain method to calibrate elasto-plastic parameters, this paper is focussed on calibrating the GTN fracture model based on a single

point based strain. The outcome of the conventional FEA updating method and the single point strain-based method (proposed in this paper) are compared.

2. Experiment set up

2.1. Material

The SS316L austenite stainless steel had a thickness of 0.1 mm and the chemical composition given in Table 1. The microstructure analysed by Scanning Electron Microscopy (SEM) with an electron backscatter diffraction (AsB) detector in the plane direction gave an average grain size of 11.2µm according to ASTM E112. The material size effects can be neglected when thickness to grain size ratio is greater than ten [7]. Thus material deformation is considered as a macro-forming process and the practical plastic theory applied.

Table 1 Average chemical composition of SS316L stainless steel determined with spectroscopy

Element	C	Cr	Ni	Mn	Si	Mo	Co
Amounts in weight %	0.06	17.38	9.56	1.47	0.56	2.11	0.15

2.2. Tensile tests

The tensile test samples were cut at 0° to the rolling direction using the slow feeding Electrical Discharge Machining technique to ensure high quality cutting edges. The samples were sprayed with a speckle paint to allow the strain field and extension displacement be measured by the GOM® Aramis [8] DIC system. Images at a frequency of 1Hz were captured by two 2448 × 2048 pixels 14 bit CCD cameras. Three tests were performed for each condition according to the ASTM E8 standard in an Instron® 30kN tensile tester. The cross-head speed was chosen to give a strain rate of $0.001s^{-1}$.

3. Numerical Analysis

3.1. Model set up

The built-in GTN model requires an Abaqus/Explicit solver. Therefore, a step time of 0.2 seconds was set to achieve a quasi-static simulation. The four-node shell elements with reduced integration (S4R) were used to mesh a quarter part of the tensile sample using symmetry boundary conditions. As it is shown in the Figure 1, a displacement boundary to simulate the pulling action of the tensile machine. The load is obtained by summing up the reaction force of nodes at the right edge of pulling region boundary. The displacement of a tip node in the pulling region was selected for output. The obtained load displacement is then doubled to consider the symmetry simplification.

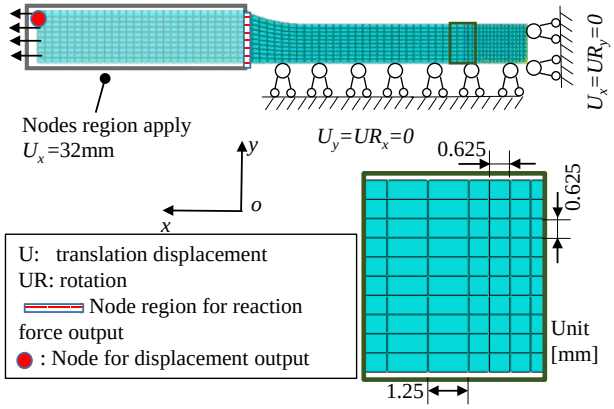

Figure 1. FEA model setup

3.2. GTN model

The GTN model is a micromechanical model where failure of the material is contributed by void nucleation, growth and coalescence. The yield function ϕ is expressed in Equation 1 with $\boldsymbol{\sigma}$ being the

component of the stress tensor and the hydrostatic pressure $p = \frac{1}{3}\mathrm{tr}(\boldsymbol{\sigma})$, in which tr(~) represents the trace of the tensor. The equivalent stress fitted by the Swift hardening law is expressed in Equation 2.

$$\phi = \left(\frac{\sigma_{eq}}{\sigma_0}\right)^2 + 2q_1 f^* \cosh\left(-\frac{3q_2 p}{2\sigma_{eq}}\right) - q_3 f^{*2} - 1 \quad (1)$$

$$\sigma_{eq} = \sigma_0 \left(1 + \frac{\varepsilon}{\varepsilon_0}\right)^n \quad (2)$$

f^* is a piecewise function and represents the effective void volume fraction f.

$$f^* = \begin{cases} f, & f \le f_c \\ f_c + \dfrac{f_u - f_c}{f_F - fc}(f - f_c), & f > f_c \end{cases} \quad (3)$$

where f_u is the ultimate value of void volume fraction, $f_u = \frac{1}{q_1}$. f_F is the void fraction where final fracture takes place. The critical void fraction f_c represents the start of void coalescence. The void volume f is the sum of the nucleation and the growth components and written in a rate form:

$$\dot{f} = \dot{f}_{Nucl} + \dot{f}_{Grow} \quad (4)$$

As the matrix volume can be assumed to be plastic incompressible, the increase of the total volume change is attributed to the void volume fraction. The void nucleation and growth rate is expressed by the equivalent plastic strain $\bar{\varepsilon}^{\mathrm{p}}$and the plastic strain tensor $\boldsymbol{\varepsilon}^{\mathrm{p}}$, respectively.

$$\dot{f}_{Growth} = (1 - f)\mathrm{tr}(\dot{\boldsymbol{\varepsilon}}^{\boldsymbol{p}}) \quad (5)$$

$$\dot{f}_{Nucl} = A(\bar{\varepsilon}^{\mathrm{p}})\mathrm{d}\bar{\varepsilon} = \frac{f_N}{S_N\sqrt{2\pi}}\exp\left[-\frac{1}{2}\left(\frac{\bar{\varepsilon}^{\mathrm{p}} - \varepsilon_N}{S_N}\right)^2\right]\mathrm{d}\bar{\varepsilon} \quad (6)$$

In summary, the GTN model contains the parameters given below:

$$\phi = G(q_1, q_2, q_3, S_N, \varepsilon_N, f_N, f_c, f_F, f_U) \quad (7)$$

Among above parameters, q_1, q_2, q_3 were introduced by Tvergaard together with the nucleation parameter S_N and can be taken from the literature [9]. f_c, f_F, f_u are the parameters that need to be identified. The Swift law (Equation 2) was fitted to the experimental true stress strain curve using Matlab. This resulted in an R square value of 99.9% (Figure 2).

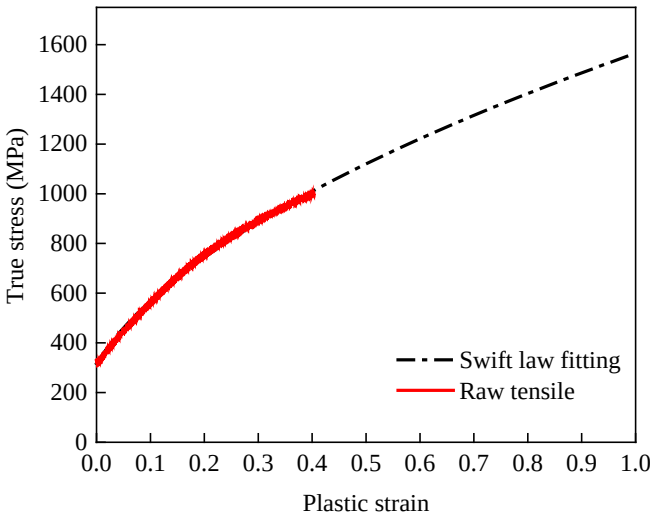

Figure 2. True stress-strain and Swift-law fitting curves determined for SS316L

Table 2. Parameters in GTN model

Parameters	q_1	q_2	q_3	S_N	ε_N	f_c	f_F	f_u	σ_0	ε_0	n
Classification	Tvergaard			Nucleation / growth		Coalescence			Swift law		
Value	1.5	1	2.25	0.3	*.	*.	*.	*.	316.7	0.047	0.516

* denotes for the parameters to be identified.

3.3. Parameter identification procedure

The calibration procedures used for the FEA updating method and the strain-based method adopt the same optimization package LS-OPT v5.1 [10]. The optimization strategy option that was used is the *sequential with domain reduction* method provided in LS-OPT. This optimization corrects each iteration by sampling a new parameter set. Correction set is sampled by D-optimal design which is controlled by regressive analysis.

3.3.1 FEA updating method:

In the FEA updating method, the optimum goal is to find the minimum error between the experimental target curve (in this case, the tensile load-displacement curve) and the numerically predicted curve. The updating method used here follows the same procedure as proposed in the literature [11]. Matlab generates a new .inp file, according to the D-optimal design, which is simulated in Abaqus (Figure 4a).

3.3.2 Strain based method:

In the strain-based method proposed here, the optimum goal is to find a set of parameters that gives the final void volume fraction f_F for fracture initiation at a critical point in the tensile gauge length, which is in the last image recorded by the DIC before fracture. The critical point is positioned in the cracking area and gives the maximum major strain at the last image recorded before fracture (Figure 3).

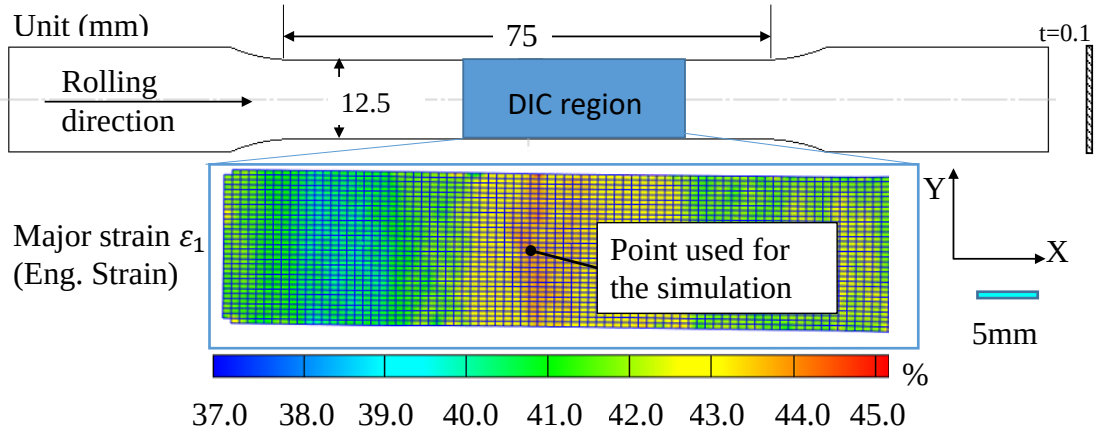

Figure 3. Major strain on the sample surface

A schematic of the proposed routine is shown in Figure 4b). In the initial step a set of parameters is guessed. Using the DIC the strain measured at the critical node (Figure 3) is split into increments of plastic strain $\Delta\boldsymbol{\varepsilon}_{t+\Delta t}$, with Δt being the interval between two sequential images, coupled with the elastic part $\Delta\boldsymbol{\varepsilon}^{e}$ and the plastic part $\Delta\boldsymbol{\varepsilon}^{p}$ of strain. The increments of strain are used in the Return Mapping (RM) algorithm to determine the stress at the single node over time. Elastic deformation is assumed and the elastically predicted stress tensor $\boldsymbol{\sigma}^{e}$ (Equation 8) relaxed onto an updated yield surface by correcting iteratively (t denotes the current time stage, $t + \Delta t$ denotes the next predicted stage). The *RM* is executed in Matlab to solve the four nonlinear Equations 8-11 and to determine the accumulated void volume fraction f at each image stage. For each iterative run, the parameter set is refreshed by LS-OPT giving a new image stage vs void fraction table, as shown in Figure 4b. The void fraction is then compared to the finial void volume fraction f_F which is the indicator for fracture.

If the solved void fraction exceedsf_F , fracture initiates and the image stage is determined as fracture stage. If this fracture stage corresponds to the last image (where fracture initiated experimentally in the tensile test) the loop stops.

$$\boldsymbol{\sigma}^{e}_{\mathrm{t}+\Delta\mathrm{t}} = \boldsymbol{\sigma}_{\mathrm{t}} + \boldsymbol{C}\colon \Delta\boldsymbol{\varepsilon}_{t+\Delta t} = \boldsymbol{\sigma}_{\mathrm{t}} + \boldsymbol{C}\colon (\Delta\boldsymbol{\varepsilon}^{\mathrm{p}} + \Delta\boldsymbol{\varepsilon}^{\mathrm{e}}) \tag{8}$$

$$\Delta\boldsymbol{\varepsilon}^{\mathrm{p}} = \frac{1}{3}\Delta\varepsilon_p\mathbf{I} + \Delta\varepsilon_q\mathbf{n} \tag{9}$$

where $\Delta\varepsilon_{\mathrm{p}} = \lambda\frac{\partial\phi}{\partial p}$; $\Delta\varepsilon_{\mathrm{q}} = \lambda\frac{\partial\phi}{\partial q}$, λ is plastic multiplier and can be contradicted in the equation manipulation. $\mathbf{I}$ is the identity tensor, $q = \sqrt{\frac{3}{2}\boldsymbol{S}\colon\boldsymbol{S}}$ and $\mathbf{S} = \boldsymbol{\sigma} - p\mathbf{I}$; Based on Equation (4) and (5), the increment of plastic strain part and void fraction can be expressed:

$$\Delta\bar{\boldsymbol{\varepsilon}}^{p} = \frac{-p\Delta\varepsilon_p + q\Delta\varepsilon_{\mathrm{q}}}{(1-f)\sigma_0} \tag{10}$$

$$\Delta f = (1-f)\Delta\varepsilon_{\mathrm{p}} + A\Delta\bar{\varepsilon}^{p} \tag{11}$$

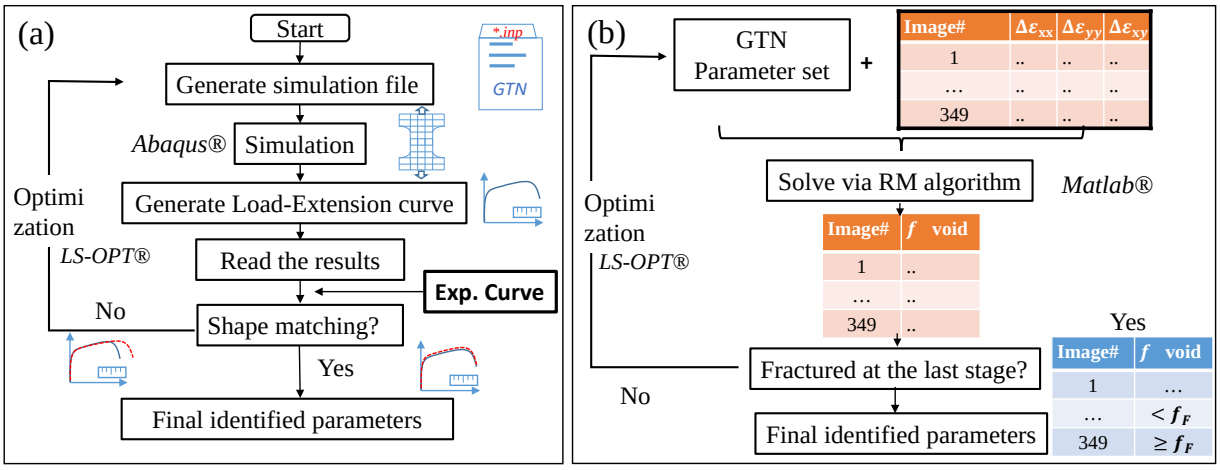

Figure 4. Flow charts of (a) FEA-updating method and b) strain-based method. The experimental input is indicated in the boxes with thicker borders.

4. Results and discussion

For the FEA updating scheme, 15 iteration and 8 runs for each iteration were required to achieve the solution. In contrast, only 9 iteration and 8 runs for each iteration were needed for the strain-based method; this was 7 times faster compared to the FEA updating scheme. Table 3 shows the final calibration results and indicates that both the FEA updating method and the new strain-based method give very similar results. This is confirmed in Figure 5, where the tensile load displacement responses achieved with the parameters identified with both methods are compared to the experimental curve. As can be seen, both methods give very similar results that correspond well with the experimental curve. It is worth to mention that different set of damage parameters could match the experimental tensile curve. Because here only one type of experiment is carried out but four unknown parameters to be determined. To obtain a unique parameters set, additional mechanical tests that provide at least three different stress state is necessary. Another way is to use the fractography assisted approach. Nonetheless, the current analysis offers an efficient way to calibrate one type of test in a short time.

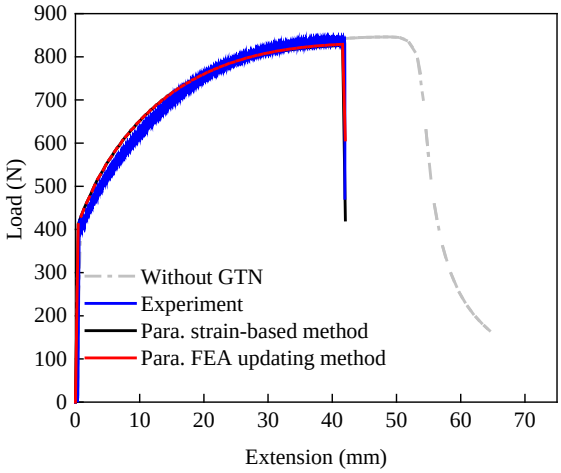

Figure 5. Calibration outcomes from simulations and experiment

Table 3. Identified results and the CPU time

	f_c	f_F	f_N	ε_N	CPU time(min)
FEA updating	0.010	0.020	0.010	0.3	423
Strain-based	0.012	0.024	0.012	0.3	65

5. Conclusion

The new strain-based calibration method proposed in this paper provides a fast solution and the resulting fracture model predictions correspond well with the experiment. In comparison, the FEA updating method achieves the same level of accuracy but at 7 times higher computational time. It should be noted that tensile test used in this study represents homogenous deformation which is rare in the real sheet metal forming process. To enhance the prediction capability of the GTN model, additional test programs which cover wide stress triaxiality are needed in future work.

Acknowledgements

The authors would like to acknowledge the financial support by the Australian Research Council (LP150100059) and the Ford (Global) Motor Company.

References

[1] Xu Z, Peng L, Fu M and Lai X 2015 *Int. J. Plast.* **68** 34–54
[2] Kleinermann J and Ponthot J 2003 *J. Mater. Process. Technol.* **139** 521–6
[3] Chaparro B, Thuillier S, Menezes L, Manach P and Fernandes J 2008 *Comput. Mater. Sci.* **44** 339–46
[4] Springmann M and Kuna M 2005 *Comput. Mater. Sci.* **33** 501–9
[5] Kim J, Serpantié A, Barlat F, Pierron F and Lee M 2013 *Int. J. Solids. Struct.* **50** 3829–42
[6] Springmann M and Kuna M 2006 *Arch. Appl. Mech.* **75** 775–97
[7] Lee R, Chen C and Gau J 2008 *Proc. Int. Conf. on Technology of Plasticity* (Seoul: Hanrimwon) pp 183–8
[8] Aramis User Manual–software 2006 GOM mbH, Germany
[9] Zhang Z 1996 *Fatigue Fract. Eng. Mater. Struct.* **19** 561–70
[10] Nielen S, Willem R, Anirban B, Trent E, Tushar G and Ken C 2015 *LS-OPT user's manual* (California:LSTC)
[11] Tsoupis I and Merklein M 2014 *Proc. 13th Int. LS-DYNA users Conf.* ed C Walton (Dearborn: LSTC) pp 1–14